AIP | Journal of Applied Physics

Enhanced room temperature electronic and thermoelectric properties of the dilute bismuthide InGaBiAs

Pernell Dongmo, Yujun Zhong, Peter Attia, Cory Bomberger, Ramez Cheaito et al.

Citation: J. Appl. Phys. **112**, 093710 (2012); doi: 10.1063/1.4761996
View online: http://dx.doi.org/10.1063/1.4761996
View Table of Contents: http://jap.aip.org/resource/1/JAPIAU/v112/i9
Published by the American Institute of Physics.

Enhanced room temperature electronic and thermoelectric properties of the dilute bismuthide InGaBiAs

Pernell Dongmo,[1] Yujun Zhong,[1] Peter Attia,[2] Cory Bomberger,[1] Ramez Cheaito,[3] Jon F. Ihlefeld,[4] Patrick E. Hopkins,[3] and Joshua Zide[1,a)]
[1]*Department of Materials Science and Engineering, University of Delaware, Newark, Delaware 19716, USA*
[2]*Department of Chemical Engineering, University of Delaware, Newark, Delaware 19716, USA*
[3]*Department of Mechanical and Aerospace Engineering, University of Virginia, Charlottesville, Virginia 2294, USA*
[4]*Sandia National Laboratories, P.O. Box 5800, M.S. 1069, Albuquerque, New Mexico 87185, USA*

(Received 14 August 2012; accepted 3 October 2012; published online 5 November 2012)

We report room temperature electronic and thermoelectric properties of Si-doped $In_{0.52}Ga_{0.48}$ Bi_yAs_{1-y} with varying Bi concentrations. These films were grown epitaxially on a semi-insulating InP substrate by molecular beam epitaxy. We show that low Bi concentrations are optimal in improving the conductivity, Seebeck coefficient, and thermoelectric power factor, possibly due to the surfactant effects of bismuth. We observed a reduction in thermal conductivity with increasing Bi concentration, which is expected because of alloy scattering. We report a peak ZT of 0.23 at 300 K. © *2012 American Institute of Physics*. [http://dx.doi.org/10.1063/1.4761996]

I. INTRODUCTION

Thermoelectric power generation (TPG) has become an increasingly popular technology for waste heat recovery in the last few years. The efficiency of TPG is essential in determining how practical this technology is in real world applications. For TPG, the efficiency is calculated using the dimensionless figure of merit, ZT, which equals to $ZT = S^2\sigma T/\kappa$, where S is the Seebeck coefficient, σ is the electrical conductivity, T is the absolute temperature, and κ is the thermal conductivity. A higher ZT leads to a higher efficiency, but increasing ZT in bulk semiconductors ($ZT \leq 1$) has proven to be difficult because of the variables' interdependence; a reduction in thermal conductivity typically leads to a reduction in electrical conductivity. Similarly, the Seebeck coefficient has an inverse relationship with electrical conductivity.

There have been several reports of increases in ZT using different techniques: incorporation of nanoparticles[1] and electron filtering.[2–7] When nanoparticles are embedded epitaxially into thin-films, the thermal conductivity is reduced past the "alloy limit" due to the increased phonon scattering. In the electron filtering technique, the Seebeck coefficient was increased (while electrical conductivity remaining relatively unchanged) by exclusively allowing high energy majority carriers (n-type: electrons) to contribute to conduction, while the low energy majority carriers are "filtered". Similarly, Heremans *et al*. were able to increase the Seebeck coefficient in PbTe by doping the films with thallium; doping with thallium caused a distortion in the density of states due to the formation of resonant energy levels.[8] In addition, it has been demonstrated that superlattices[9] can enhance the ZT relative to their bulk material due to effectively reducing the lattice thermal conductivity, especially at low temperatures. For bulk materials, $ZT \sim 1.5$ has been reported at 700 K in $AgPb_{18}SbTe_{20}$ due to the presence of "nanodots."[10] Finally, Shi *et al*. demonstrated that double-filled skutterudites (n-$Ba_xYb_yCo_4Sb_{12}$) had a reduced thermal conductivity because of the effective phonon scattering from Ba and Yb, which led to a peak ZT of 1.36 at 800 K.[11] More detail about the effects of nanostructures on thermoelectric properties can be found elsewhere.[12]

Dilute bismuthides ($In_xGa_{1-x}Bi_yAs_{1-y}$) are relatively new and promising materials for thermoelectrics because of the expected decrease in thermal conductivity due to alloying and bismuth being a heavy atom (better phonon scattering). In addition, since InGaAs has moderately high thermoelectric power factor (TPF), a similar TPF in dilute bismuthides should be achievable because of an InGaAs-like conduction band. There have been many reports on GaBiAs,[13–19] but relatively few on InGaBiAs. Petropoulos *et al*. discussed the optical and electronic properties of undoped dilute bismuthides.[20] Devenson *et al*. also investigated the structural and optical properties of undoped InGaBiAs that contained up to 7% Bi.[21] Zhong *et al*. discussed the optimum growth conditions required for Bi incorporation.[22] While most of the focus has been on undoped dilute bismuthides, the electronic and thermoelectric properties of doped (n-type) dilute bismuthides have yet to be published. In this paper, we present the room temperature electronic and thermoelectric properties of n-InGaBiAs, along with the corresponding thermoelectric figure of merit. Additionally, we report on heavily doped samples, for which extremely high carrier concentrations and electrical conductivity were achieved.

II. GROWTH AND SAMPLE CHARACTERIZATION

All samples mentioned in this paper were grown using a OSEMI NextGen molecular beam epitaxy (MBE) system on (001) InP:Fe substrates. A more detailed description of the growth conditions can be found elsewhere.[22] The sample structure consists of 70 nm $In_{0.53}Ga_{0.47}As$ followed by 300 nm Si:$In_{0.52}Ga_{0.48}Bi_xAs_{1-x}$. All samples were grown at a growth temperature of 300 °C, under an As overpressure

a)Electronic mail: zide@udel.edu.

(As beam equivalent pressure or BEP = 2×10^{-6}); growth temperature is monitored by band-edge thermometry. The Bi flux (Bi BEP = 1×10^{-8}, corresponding to1.6% Bi) is held constant for each set of samples, while the silicon cell temperature varies from 1100 °C to 1390 °C. We also grew samples with higher Bi concentrations (Bi BEP = 1.5×10^{-8}, 2.0×10^{-8}, which corresponds to 2.6% Bi and 4.4% Bi, respectively) with a silicon cell temperature of 1200 °C, 1215 °C, and 1245 °C.

The carrier concentration, mobility, and conductivity for each sample were obtained by a custom-built Hall Effect system using Van der Pauw geometry. Each sample was cleaved to 1 cm × 1 cm square with indium contacts deposited on each corner.

We also measured the Seebeck coefficient of each sample. Each sample was cleaved to a 6 mm × 15 mm bar with a strip of indium deposited (via soldering iron) on each end (thickness ~ 1 mm) for contacts. The sample bar is then thermally pasted onto two Peltier modules that are ~1 cm apart; one module is heated and the other is cooled. Type K thermocouples are placed on each end (on top of indium contacts) to measure ΔT, along with two copper probes to measure voltage. The temperature difference was varied by controlling the power applied to the Peltier modules. The Seebeck coefficient is the slope of the resulting V vs. ΔT curve, which is linear.

We measure the thermal conductivity of the various bismuthide samples with time domain thermoreflectance (TDTR).[23] In short, TDTR is a pump-probe technique in which laser pulses emanate from a Ti:sapphire oscillator. We delay the time in which the probe pulses reach the sample with respect to the pump pulses with a mechanical delay stage that gives ~6 ns of probe delay. For this study, we modulate the pump path at 11 MHz with a linearly amplified sinusoid and monitor the ratio of the in-phase to out-of-phase signal of the probe beam with a lock-in amplifier. Prior to TDTR measurements, we coat the samples with a thin Al or Pt film transducer. To determine the thermal conductivity of the bismuthide samples, we fit the TDTR data to a multi-layer thermal model that has been detailed by several groups elsewhere.[24–26] We assume literature values for the heat capacities of the metal transducer and the substrate.[27–29] We calculate the heat capacity of the samples by averaging the heat capacity of $In_{0.55}Ga_{0.45}As$[30] and Bi.[27] The thermal conductivity of the Al or Pt transducers is approximated from electrical resistivity measurements, although over the time delay during our TDTR measurements, we are relatively insensitive to the thermal conductivity of the metal transducer. We fit the TDTR model to the data by varying the thermal conductivity of the bismuthide films. We also slightly adjust the thermal boundary conductance between the metal and the bismuthide samples, but due to the relatively low values of thermal conductivity of the samples, we are much more sensitive to small changes in the values of thermal conductivity than the thermal boundary conductance, thereby reducing the uncertainty in determining the thermal conductivity of the alloy films. Due to the thickness of the samples and their relatively low thermal conductivity compared to the thermal penetration depth of our laser at 11 MHz, we are insensitive to the thermal boundary conductance between the bismuthide and the substrate.

III. RESULTS AND DISCUSSION

A plot of electrical conductivity versus carrier concentration is shown in Fig. 1(a). The highest electrical

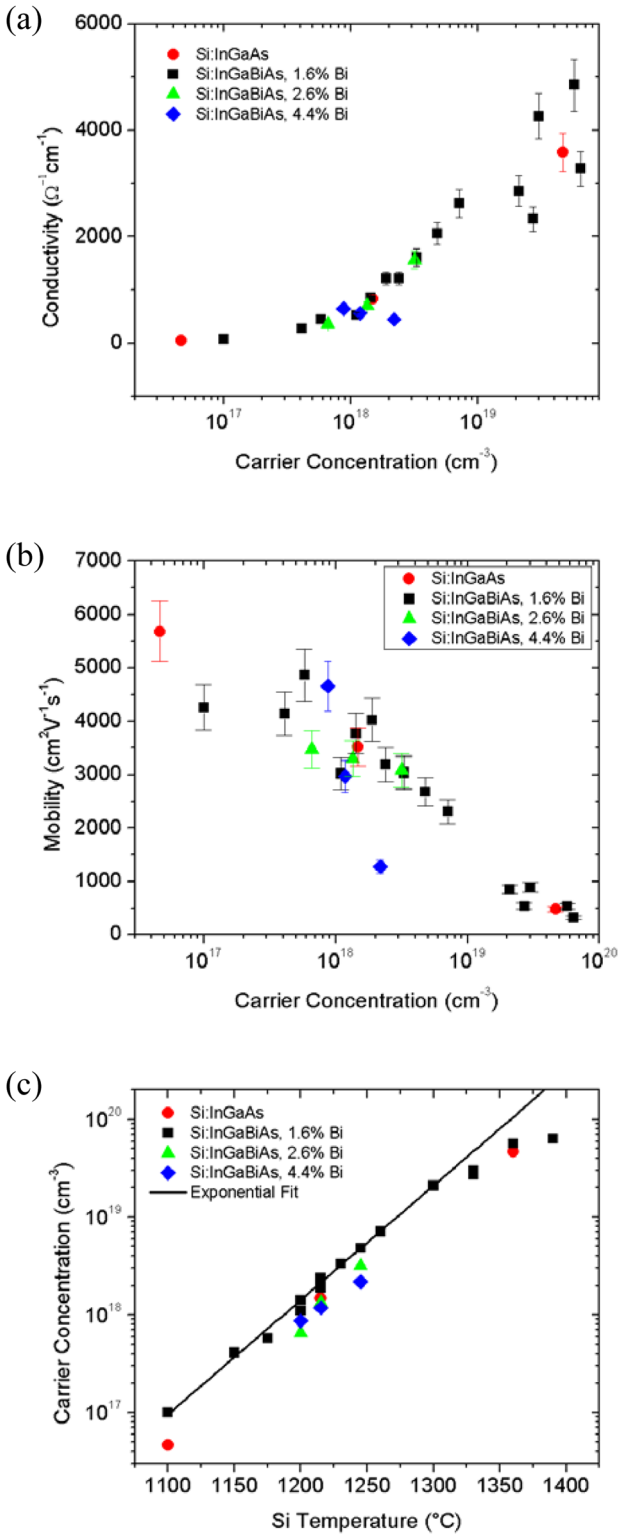

FIG. 1. (a) Electrical conductivity and (b) mobility of Si:InGaAs (circle), $Si:In_{0.52}Ga_{0.48}Bi_{.016}As_{.984}$ (square), $Si:InGaBi_{.026}As_{.974}$ (triangle), and $Si:InGaBi_{.044}As_{.956}$ vs carrier concentration. (c) Carrier concentration of previously mentioned films vs Si temperature (°C). The solid line represents an exponential fit of $Si:In_{0.52}Ga_{0.48}Bi_{.016}As_{.984}$ from 1100 °C to 1300 °C. There is some uncertainty in the Hall measurements due to the ratio between the diameter of the indium contact to the length of the sample side.

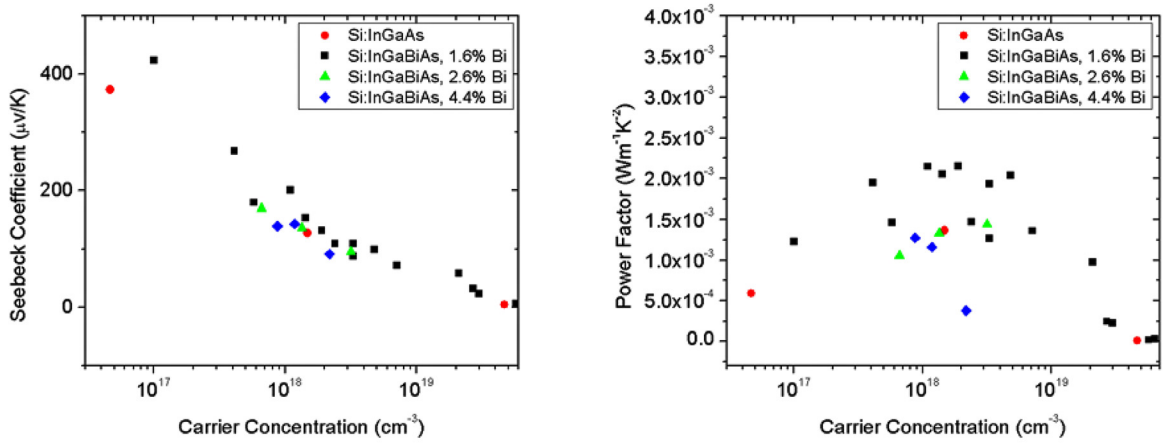

FIG. 2. (a) Seebeck coefficient and (b) TPF of Si:InGaAs (circle), Si:$In_{0.52}Ga_{0.48}Bi_{.016}As_{.984}$ (square), Si:$InGaBi_{.026}As_{.974}$ (triangle), and Si:$InGaBi_{.044}As_{.956}$ vs carrier concentration.

conductivity we recorded was 4850 S/cm, which is quite high for a semiconductor material. A few samples with high carrier concentration have relatively low conductivity due to reduced mobility, presumably due to lower material quality. Mobility versus carrier concentration is shown in Fig. 1(b). Incorporating of small concentrations of Bi into Si:InGaAs does not significantly reduce mobility. Finally, Fig. 1(c) shows a plot of carrier concentration as a function of silicon cell temperature. The highest carrier concentration measured was $6.4 \times 10^{19}\,cm^{-3}$. At 1.6%Bi, the carrier concentration increases (compared to Si:InGaAs); at higher Bi concentrations, the carrier concentrations drop slightly below Si:InGaAs. This seems to suggest that there is an optimum Bi concentration ($0 < y < .026$) in which the maximum carrier concentration can be achieved for Si: $In_{0.52}Ga_{0.48}Bi_yAs_{1-y}$. A possible explanation for this observation is that bismuth is known to be a surfactant, which helps improve the overall film quality, but it may also create a large density of step edges, allowing easier silicon adsorption.[16] As a result, at low concentrations, more silicon can be incorporated into the InGaBiAs matrix. At higher concentrations, bismuth may hinder silicon incorporation, explaining the small reduction in carrier concentration in samples with more bismuth.

Figure 2 shows the Seebeck coefficient (a) and TPF (b) vs carrier concentration. At 1.6% Bi, there is an improvement in Seebeck coefficient and TPF, relative to Si:InGaAs, especially at low to moderate carrier concentrations of n-InGaBiAs. For example, at a carrier concentration of $\sim 1.4 \times 10^{-18}\,cm^{-3}$, we see a 49.6% improvement in TPF from Si:InGaAs ($1.37 \times 10^{-3}\,Wm^{-1}\,K^{-1}$) to Si:$In_{0.52}Ga_{0.48-}Bi_{.016}As_{.984}$ ($2.05 \times 10^{-3}\,Wm^{-1}\,K^{-1}$). The improvement results from a larger Seebeck coefficient, which could result from a more complex conduction band profile in these materials. This is an unexpected result, as the conduction band was not believed to differ significantly from InGaAs in these materials. At 2.6% Bi, there is negligible improvement in both the Seebeck coefficient and TPF, and at 4.4% Bi, the thermoelectric properties are slightly worse.

There is some error in Seebeck measurements albeit small. The temperature measurement, which is the largest source of error, is estimated to be ± 1 K. This error is due to the thermal contact between the sample and the indium metal. The Seebeck coefficient was obtained by measuring the slope of five different (ΔT, V) points; the R^2 for the linear fit was ~ 1. Also, there is negligible contribution in conduction between the film and substrate.

Thermal conductivity measurements were performed on a variety of samples with varying Bi concentration, including some of the previously stated Si:InGaBiAs, which were all grown under similar growth conditions as mentioned previously. The measurements are plotted as a function of %Bi in Figure 3. There is a general downward trend in thermal conductivity with increasing Bi concentration, which is expected from alloy scattering. For Si:InGaAs, one sample had a relatively high thermal conductivity. Using Wiedemann-Franz Law, we determined that roughly 40% of the total thermal conductivity was from electronic contribution; if we neglect the electronic contribution, the thermal conductivity of that sample would fall within the range of the other samples. The electronic contribution from the other Si:InGaAs samples is

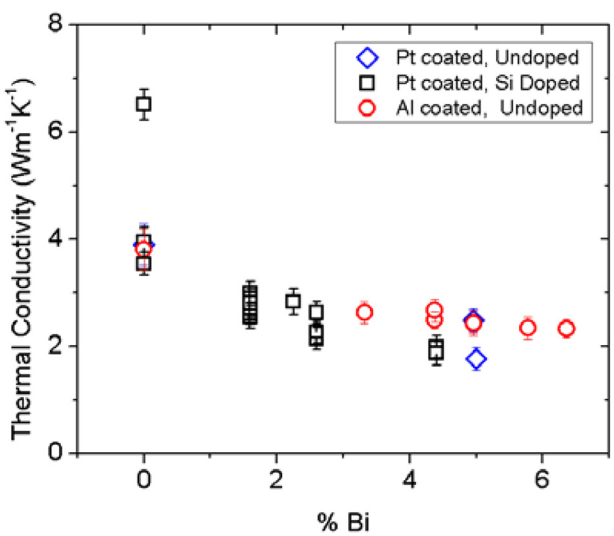

FIG. 3. Thermal conductivity vs %Bi for $In_xGa_{1-x}Bi_yAs_{1-y}$ and Si:$In_xGa_{1-x}Bi_yAs_{1-y}$. All Al coated samples (circle) were $In_xGa_{1-x}Bi_yAs_{1-y}$. The Pt coated samples were mostly Si:$In_xGa_{1-x}Bi_yAs_{1-y}$ (square) and some $In_xGa_{1-x}Bi_yAs_{1-y}$ (diamond, Bi% = 0, 4.96, 5).

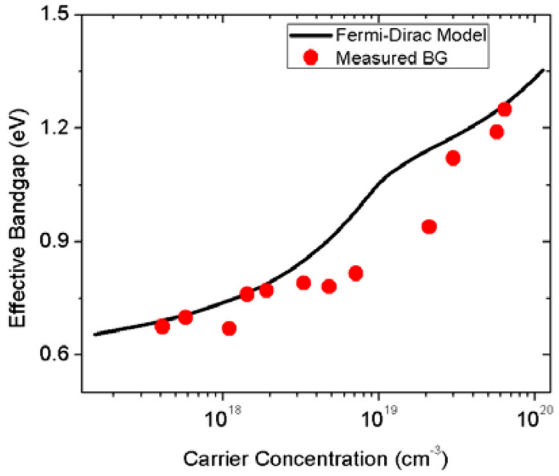

FIG. 4. Effective bandgap (due to band filling) vs carrier concentration of Si:$In_{0.52}Ga_{0.48}Bi_{.016}As_{.984}$. The model was based on the calculation of the Fermi-Dirac integral for an InGaAs conduction band.

significantly smaller. The error bars represent the uncertainty calculated due to the metal film thickness and the standard deviation about the mean of the various measurements on each sample.

A Burstein-Moss shift[31,32] was also observed in Si:InGaBiAs. A plot of the effective bandgap vs carrier concentration can be seen in Figure 4. The model is based on the Fermi-Dirac integral for InGaAs, assuming multiple parabolic conduction bandgap (Γ-valley and L-valley) and a flat valence band. Comparing the model to our measured bandgap values, we see that the conduction band of Si:InGaBiAs is reasonably similar to that of InGaAs. The differences might be explained by a change in the conduction band from that of InGaBiAs.

IV. SUMMARY AND CONCLUSIONS

In summary, incorporating low concentrations of bismuth into Si:InGaAs has proven to be beneficial from an electric/thermoelectric point of view. Compared to silicon doped InGaAs, it has shown to improve conductivity and Seebeck coefficient while maintaining a relatively high mobility, which leads to an improvement in TPF. We also observe remarkably high conductivity and carrier concentration in heavily-doped samples. However, a higher bismuth concentration (>2.4% Bi) can become somewhat detrimental to the electronic and thermoelectric properties of the material. As expected, we see a reduction in thermal conductivity with increasing bismuth concentrations. We achieved a peak ZT of 0.23, which, though unexceptional, is encouraging; this is a large value for III-V materials, and we expect a higher ZT at higher temperatures because increasing temperatures yield a higher power factor, lower thermal conductivity, and a larger T. Since the electrical properties of these films are isotropic, the cross-plane electrical conductivity or Seebeck coefficient is not necessary in the calculation of ZT. Based on these results, dilute bismuthides remain promising for thermoelectric power generation at moderate temperature.

ACKNOWLEDGMENTS

The authors would like to acknowledge the financial support of the Office of Naval Research through the Young Investigator Program.

[1]W. Kim, J. Zide, A. Gossard, D. Klenov, S. Stemmer, A. Shakouri, and A. Majumdar, Phys. Rev. Lett. **96**, 045901 (2006).
[2]J. Zide, D. Vashaee, Z. Bian, G. Zeng, J. Bowers, A. Shakouri, and A. C. Gossard, Phys. Rev. B **74**, 1–5 (2006).
[3]G. Mahan and L. Woods, Phys. Rev. Lett. **80**, 4016–4019 (1998).
[4]D. Vashaee and A. Shakouri, Phys. Rev. Lett. **92**, 10–13 (2004).
[5]C. B. Vining and G. D. Mahan, J. Appl. Phys. **86**, 6852 (1999).
[6]D. Vashaee, J. Appl. Phys. **95**, 1233 (2004).
[7]J. M. O. Zide, J.-H. Bahk, R. Singh, M. Zebarjadi, G. Zeng, H. Lu, J. P. Feser, D. Xu, S. L. Singer, Z. X. Bian, A. Majumdar, J. E. Bowers, A. Shakouri, and A. C. Gossard, J. Appl. Phys. **108**, 123702 (2010).
[8]J. P. Heremans, V. Jovovic, E. S. Toberer, A. Saramat, K. Kurosaki, A. Charoenphakdee, S. Yamanaka, and G. J. Snyder, Science **321**, 554–557 (2008).
[9]R. Venkatasubramanian, E. Siivola, T. Colpitts, and B. O'Quinn, Nature **413**, 597–602 (2001).
[10]K. F. Hsu, S. Loo, F. Guo, W. Chen, J. S. Dyck, C. Uher, T. Hogan, E. K. Polychroniadis, and M. G. Kanatzidis, Science **303**, 818–821 (2004).
[11]X. Shi, H. Kong, C.-P. Li, C. Uher, J. Yang, J. R. Salvador, H. Wang, L. Chen, and W. Zhang, Appl. Phys. Lett. **92**, 182101 (2008).
[12]C. J. Vineis, A. Shakouri, A. Majumdar, and M. G. Kanatzidis, Adv. Mater. **22**, 3970–3980 (2010).
[13]Y. Tominaga, Y. Kinoshita, K. Oe, and M. Yoshimoto, Appl. Phys. Lett. **93**, 131915 (2008).
[14]S. Tixier, M. Adamcyk, T. Tiedje, S. Francoeur, A. Mascarenhas, P. Wei, and F. Schiettekatte, Appl. Phys. Lett. **82**, 2245 (2003).
[15]X. Lu, D. A. Beaton, R. B. Lewis, T. Tiedje, and M. B. Whitwick, Appl. Phys. Lett. **92**, 192110 (2008).
[16]A. Duzik, J. C. Thomas, J. M. Millunchick, J. Lång, M. P. J. Punkkinen, and P. Laukkanen, Surf. Sci. **606**, 1203–1207 (2012).
[17]K. Alberi, J. Wu, W. Walukiewicz, K. Yu, O. Dubon, S. Watkins, C. Wang, X. Liu, Y.-J. Cho, and J. Furdyna, Phys. Rev. B **75**, 1–6 (2007).
[18]K. Bertulis, A. Krotkus, G. Aleksejenko, V. Pačebutas, R. Adomavičius, G. Molis, and S. Marcinkevičius, Appl. Phys. Lett. **88**, 201112 (2006).
[19]A. J. Ptak, R. France, D. A. Beaton, K. Alberi, J. Simon, A. Mascarenhas, and C.-S. Jiang, J. Cryst. Growth **338**, 107–110 (2012).
[20]J. P. Petropoulos, Y. Zhong, and J. M. O. Zide, Appl. Phys. Lett. **99**, 031110 (2011).
[21]J. Devenson, V. Pačebutas, R. Butkutė, A. Baranov, and A. Krotkus, Appl. Phys. Express **5**, 015503 (2012).
[22]Y. Zhong, P. B. Dongmo, J. P. Petropoulos, and J. M. O. Zide, Appl. Phys. Lett. **100**, 112110 (2012).
[23]D. G. Cahill, K. E. Goodson, and A. Majumdar, J. Heat Transfer **124**, 223–241 (2002).
[24]P. E. Hopkins *et al.*, J. Heat Transfer **132**, 081302 (2010).
[25]A. J. Schmidt, X. Chen, and G. Chen, Rev. Sci. Instrum. **79**, 114902 (2008).
[26]D. G. Cahill, Rev. Sci. Instrum. **75**(12), 5119–5122 (2004).
[27]Y. S. Touloukian and E. H. Buyco, *Thermophysical Properties of Matter – Specific Heat: Metallic Elements and Alloys* (IFI/Plenum, New York, 1970), Vol. 4.
[28]Y. S. Touloukian *et al.*, *Thermophysical Properties of Matter – Specific Heat: Nonmetallic Solids* (IFI/Plenum, New York, 1970), Vol. 5.
[29]Y. S. Touloukian *et al.*, *Thermophysical Properties of Matter – Thermal Conductivity: Nonmetallic Solids*. (IFI/Plenum, New York, 1970), Vol. 2.
[30]S. Adachi, *Physical Properties of III-V Semiconductor Compounds: InP, In As, GaAs, GaP, InGaAs, and InGaAsP* (Wiley-VCH, Weinheim, 2004).
[31]E. Burstein, Phys. Rev. **93**(3), 632–633 (1954).
[32]T. S. Moss, Proc. Phys. Soc. **67**, 775, (1954).